

Spectral and Thermal Properties of Ho³⁺ Doped in Zinc Lithium Alumino Antimony Borophosphate Glasses

Dr. S.L.Meena

Assistant Professor
Ceramic Laboratory,
Department of physics,
Jai Narain Vyas University, Jodhpur 342001(Raj.) India

Abstract: Glass of the system: (35-x) P₂O₅:10ZnO:10Li₂O:10Al₂O₃:15Sb₂O₃:20B₂O₃: xHo₂O₃. (where x=1, 1.5, 2 mol %) have been prepared by melt-quenching method. (where x=1, 1.5 and 2 mol%) have been prepared by melt-quenching technique. The amorphous nature of the prepared glass samples was confirmed by X-ray diffraction. Optical absorption and fluorescence spectra were recorded at room temperature for all glass samples. Judd-Ofelt intensity parameters Ω_λ ($\lambda=2, 4$ and 6) are evaluated from the intensities of various absorption bands of optical absorption spectra. Using these intensity parameters various radiative properties like spontaneous emission probability, branching ratio, radiative life time and stimulated emission cross-section of various emission lines have been evaluated

Keywords: ZLAABP Glasses, Optical Properties, Judd-Ofelt Theory, Thermal Properties.

I. Introduction

Glasses containing rare-earth (RE) ions such as Pr³⁺, Nd³⁺, Er³⁺, Ho³⁺ and Sm³⁺ ions have received much attention, because such materials have high potential for practical applications [1-5]. Phosphate glasses possess easier preparation, large transparency window, low phonon energy, better thermal stability, high refractive index, and chemical durability [6-10]. Ho³⁺ doped glasses are very important because of the possibility of their application in optoelectronic, optic device fields, such as lasers, fiber optic large bandwidth, high emission and absorption cross-section and solar cells [11-13]. ZnO is a wide band gap semiconductor and has received increasing research interest. It is an important multifunction material due to its specific chemical, surface and micro structural properties. The addition of network modifier (NWF) Li₂O is to improve both electrical and mechanical properties of such glasses. Recently, rare earth doped phosphate glass has attracted much interest because of high rare earth ion solubility, optical data transmission, detection and sensing [14, 15].

The present work reports on the preparation and characterization of rare earth doped heavy metal oxide (HMO) glass systems for lasing materials. We have studied on the absorption and emission properties of Ho³⁺ doped zinc lithium alumino antimony borophosphate glasses. The intensities of the transitions for the rare earth ions have been estimated successfully using the Judd-Ofelt theory, The laser parameters such as radiative probabilities(A), branching ratio (β), radiative life time(τ_R) and stimulated emission cross section(σ_p) are evaluated using J.O.intensity parameters(Ω_λ , $\lambda=2, 4$ and 6).

II. Experimental Techniques

Preparation of glasses

The following Ho³⁺ doped Borophosphate glass samples (35-x) P₂O₅:10ZnO:10Li₂O:10Al₂O₃:15Sb₂O₃:20B₂O₃: xHo₂O₃. (where x=1, 1.5 and 2 mol%) have been prepared by melt-quenching method. Analytical reagent grade chemical used in the present study consist of P₂O₅, ZnO, Li₂O, Al₂O₃, Sb₂O₃, B₂O₃ and Ho₂O₃. They were thoroughly mixed by using an agate pestle mortar. then melted at 1060°C by an electrical muffle furnace for 2h., After complete melting, the melts were quickly poured in to a preheated stainless steel mould and annealed at temperature of 260°C for 2h to remove thermal strains and stresses. Every time fine powder of cerium oxide was used for polishing the samples. The glass samples so prepared were of good optical quality and were transparent. The chemical compositions of the glasses with the name of samples are summarized in **Table 1**.

Table 1.

Chemical composition of the glasses

Sample	Glass composition (mol %)
ZLAABP (UD)	35 P ₂ O ₅ :10ZnO:10Li ₂ O:10Al ₂ O ₃ :15Sb ₂ O ₃ :20B ₂ O ₃
ZLAABP (HO1)	34 P ₂ O ₅ :10ZnO:10Li ₂ O:10Al ₂ O ₃ :15Sb ₂ O ₃ :20B ₂ O ₃ :1 Ho ₂ O ₃
ZLAABP (HO1.5)	33.5 P ₂ O ₅ :10ZnO:10Li ₂ O:10Al ₂ O ₃ :15Sb ₂ O ₃ :20B ₂ O ₃ :1.5 Ho ₂ O ₃
ZLAABP (HO2)	33 P ₂ O ₅ :10ZnO:10Li ₂ O:10Al ₂ O ₃ :15Sb ₂ O ₃ :20B ₂ O ₃ : 2 Ho ₂ O ₃

ZLAABP (UD) -Represents undoped Zinc Lithium Alumino Antimony Borophosphate glasses specimens.

ZLAABP (HO) -Represents Ho³⁺ doped Zinc Lithium Alumino Antimony Borophosphate glass specimens.

III. Theory

3.1 Oscillator Strength

The intensity of spectral lines are expressed in terms of oscillator strengths using the relation [16].

$$f_{\text{expt.}} = 4.318 \times 10^{-9} \int \epsilon(\nu) d\nu \tag{1}$$

where, $\epsilon(\nu)$ is molar absorption coefficient at a given energy ν (cm^{-1}), to be evaluated from Beer–Lambert law.

Under Gaussian Approximation, using Beer–Lambert law, the observed oscillator strengths of the absorption bands have been experimentally calculated [17], using the modified relation:

$$P_m = 4.6 \times 10^{-9} \times \frac{1}{cl} \log \frac{I_0}{I} \times \Delta\nu_{1/2} \tag{2}$$

where c is the molar concentration of the absorbing ion per unit volume, l is the optical path length, $\log I_0/I$ is optical density and $\Delta\nu_{1/2}$ is half band width.

3.2. Judd-Ofelt Intensity Parameters

According to Judd [18] and Ofelt [19] theory, independently derived expression for the oscillator strength of the induced forced electric dipole transitions between an initial J manifold $|4f^N(S, L) J\rangle$ level and the terminal J' manifold $|4f^N(S', L') J'\rangle$ is given by:

$$\frac{8\pi^2 m c \nu}{3h(2J+1)n} \frac{1}{n} \left[\frac{(n^2+2)^2}{9} \right] \times S(J, J') \tag{3}$$

Where, the line strength $S(J, J')$ is given by the equation

$$S(J, J') = e^2 \sum_{\lambda=2, 4, 6} \Omega_\lambda \langle 4f^N(S, L) J || U^{(\lambda)} || 4f^N(S', L') J' \rangle^2 \tag{4}$$

In the above equation m is the mass of an electron, c is the velocity of light, ν is the wave number of the transition, h is Planck's constant, n is the refractive index, J and J' are the total angular momentum of the initial and final level respectively, Ω_λ ($\lambda=2, 4$ and 6) are known as Judd-Ofelt intensity.

3.3 Radiative Properties

The Ω_λ parameters obtained using the absorption spectral results have been used to predict radiative properties such as spontaneous emission probability (A) and radiative life time (τ_R), and laser parameters like fluorescence branching ratio (β_R) and stimulated emission cross section (σ_p).

The spontaneous emission probability from initial manifold $|4f^N(S', L') J'\rangle$ to a final manifold $|4f^N(S, L) J\rangle$ is given by:

$$A[(S', L') J'; (S, L) J] = \frac{64 \pi^2 \nu^3}{3h(2J'+1)} \left[\frac{n(n^2+2)^2}{9} \right] \times S(J', J) \tag{5}$$

Where, $S(J', J) = e^2 [\Omega_2 || U^{(2)} ||^2 + \Omega_4 || U^{(4)} ||^2 + \Omega_6 || U^{(6)} ||^2]$

The fluorescence branching ratio for the transitions originating from a specific initial manifold $|4f^N(S', L') J'\rangle$ to a final manifold $|4f^N(S, L) J\rangle$ is given by

$$\beta[(S', L') J'; (S, L) J] = \frac{A[(S', L') J'; (S, L) J]}{\sum_{S, L, J} A[(S', L') J'; (S, L) J]} \tag{6}$$

where, the sum is over all terminal manifolds.

The radiative life time is given by

$$\tau_{rad} = \sum_{S, L, J} A[(S', L') J'; (S, L) J] = A_{Total}^{-1} \tag{7}$$

where, the sum is over all possible terminal manifolds. The stimulated emission cross-section for a transition from an initial manifold $|4f^N(S', L') J'\rangle$ to a final manifold $|4f^N(S, L) J\rangle$ is expressed as

$$\sigma_p(\lambda_p) = \left[\frac{\lambda_p^4}{8\pi c n^2 \Delta\lambda_{eff}} \right] \times A[(S', L') J'; (\bar{S}, \bar{L}) \bar{J}] \tag{8}$$

where, λ_p the peak fluorescence wavelength of the emission band and $\Delta\lambda_{eff}$ is the effective fluorescence line width.

3.4 Nephelauxetic Ratio (β') and Bonding Parameter ($b^{1/2}$)

The nature of the R-O bond is known by the Nephelauxetic Ratio (β') and Bonding Parameters ($b^{1/2}$), which are computed by using following formulae [20, 21]. The Nephelauxetic Ratio is given by

$$\beta' = \frac{\nu_g}{\nu_a} \tag{9}$$

where, ν_a and ν_g refer to the energies of the corresponding transition in the glass and free ion, respectively. The value of bonding parameter ($b^{1/2}$) is given by

$$b^{1/2} = \left[\frac{1-\beta'}{2} \right]^{1/2} \tag{10}$$

IV. Result and Discussion

4.1 XRD Measurement

Figure 1 presents the XRD pattern of the sample contain - P_2O_5 which is show no sharp Bragg's peak, but only a broad diffuse hump around low angle region. This is the clear indication of amorphous nature within the resolution limit of XRD instrument.

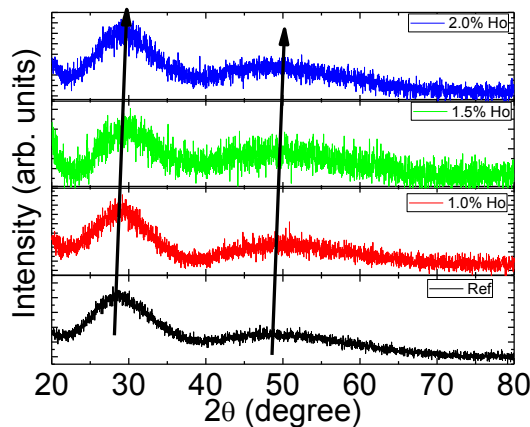


Fig. 1 X-ray diffraction pattern of P_2O_5 : ZnO: Li_2O : Al_2O_3 : Sb_2O_3 : B_2O_3 : Ho_2O_3

4.2. Thermal Studies

Fig. 2 depicts the DTA thermogram of powdered ZLAABP sample show an endothermic peak corresponding to glass transition event followed by an exothermic peak related to crystallization event. The glass transition temperature (T_g), onset crystallization temperature (T_x), crystallization temperature (T_c) were estimated to be $515^{\circ}C$, $585^{\circ}C$ and $612^{\circ}C$ respectively. From the measured value of T_g , T_x and T_c , the glass stability factor ($\Delta T = T_x - T_g$) has been determined to be $70^{\circ}C$ indicating the good stability of the glass. Therefore, the present glass composition could also be used to draw fiber and used to determine the required heat temperatures applied to induce crystallization.

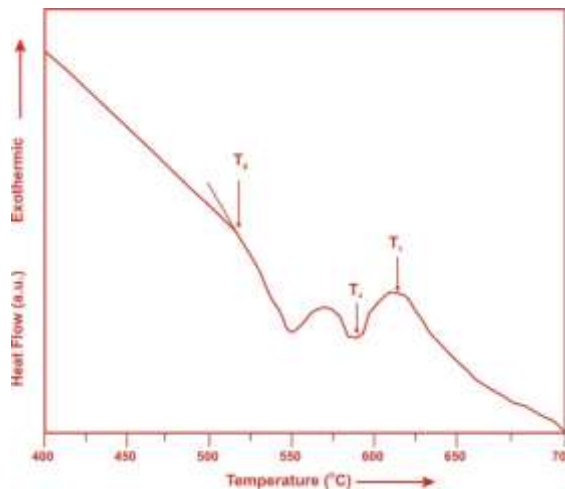


Fig. 2. DTA thermogram of powdered ZLAABP sample.

Obtained results indicate that by increasing the amount of mol% Ho₂O₃, the T_g of the samples also increases, the small increase of T_g in these glasses shows that the structure is strongly and progressively modified. The thermal stabilities ΔT of the ZLAABP reference glass and Ho³⁺doped ZLAABP glass has been evaluated from their T_g, T_c and T_c values, the results are listed out in Table 2. Hruby's parameter also calculated by using eq. (11), the greater values of the Hruby's parameter indicate higher glass forming tendency, the values of H in our glasses increased with the addition of the Ho₂O₃. Eqs. (12) and (13) present the GS parameter of Weinberg [22] and Lu and Liu [23], respectively.

$$H = \frac{T_X - T_g}{T_c - T_X} \tag{11}$$

$$K_W = \frac{T_X - T_g}{T_c} \tag{12}$$

$$K_{LL} = \frac{T_X}{T_g + T_c} \tag{13}$$

Table 2: Thermal parameters determined from the DTA traces of ZLAABP (HO) glasses.

Sample Name	% Ho ₂ O ₃	T _g ⁰ C	T _X ⁰ C	T _c ⁰ C	ΔT	H	K _W	K _{LL}
ZLAABP (HO 1.0)	1	515	585	612	70	2.59	0.1144	0.5191
ZLAABP (HO 1.5)	1.5	517	588	615	71	2.63	0.1155	0.5194
ZLAABP (HO 02)	2	520	592	619	72	2.67	0.1163	0.5198

4.3 Absorption Spectrum

The absorption spectra of Ho³⁺doped ZLAABP glass specimens have been presented in Figure 3 in terms of optical density versus wavelength. Twelve absorption bands have been observed from the ground state ⁵I₈ to excited states ⁵I₅, ⁵I₄, ⁵F₅, ⁵F₄, ⁵F₃, ³K₈, ⁵G₆, (⁵G, ³G)₅, ⁵G₄, ⁵G₂, ⁵G₃, and ³F₄ for Ho³⁺ doped ZLAABP glasses.

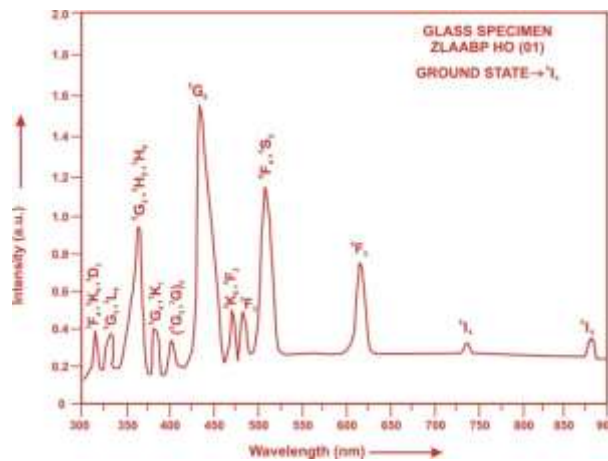


Fig. (3) Absorption spectrum of Ho³⁺doped ZLAABP glasses.

The experimental and calculated oscillator strength for Ho³⁺ ions in ZLAABP glasses are given in **Table 3**.

Table 3: Measured and calculated oscillator strength ($P_m \times 10^{+6}$) of Ho³⁺ ions in ZLAABP glasses.

Energy level from ⁵ I ₈	Glass ZLAABP(HO01)		Glass ZLAABP (HO1.5)		Glass ZLAABP (HO02)	
	P _{exp.}	P _{cal.}	P _{exp.}	P _{cal.}	P _{exp.}	P _{cal.}
⁵ I ₅	0.48	0.24	0.45	0.24	0.42	0.24
⁵ I ₄	0.06	0.02	0.05	0.02	0.03	0.02
⁵ F ₅	3.65	2.79	3.61	2.76	3.55	2.73
⁵ F ₄	4.68	4.35	4.63	4.31	4.58	4.25
⁵ F ₃	1.58	2.42	1.55	2.40	1.51	2.37
³ K ₈	1.45	1.99	1.40	1.96	1.36	1.93
⁵ G ₆	25.68	25.64	24.98	24.97	23.75	23.76
(⁵ G, ³ G) ₅	3.76	1.68	3.72	1.66	3.68	1.63
⁵ G ₄	0.08	0.61	0.06	0.60	0.05	0.59
⁵ G ₂	5.75	5.45	5.72	5.33	5.68	5.10
⁵ G ₃	1.54	1.40	1.51	1.38	1.45	1.35
³ F ₄	1.40	4.14	1.35	4.09	1.30	4.02
r.m.s. deviation	±1.08552		±1.08551		±1.08505	

*Low r.m.s.deviation values clearly indicate the accuracy of fitting.

Computed values of F₂, Lande's parameter (ξ_{4f}), Nephelauxetic ratio (β') and bonding parameter ($b^{1/2}$) for Ho³⁺ ions in ZLAABP glass specimen are given in Table 4.

Table 4: F₂, ξ_{4f} , β' and $b^{1/2}$ parameters for Holmium doped glass specimen.

Glass Specimen	F ₂	ξ_{4f}	β'	$b^{1/2}$
Ho ³⁺	358.82	1258.16	0.9337	0.1821

In the Zinc Lithium Alumino Antimony Borophosphate glasses (ZLAABP) Ω_2 , Ω_4 and Ω_6 parameters decrease with the increase of x from 1 to 2 mol%. The order of magnitude of Judd-Ofelt intensity parameters is $\Omega_2 > \Omega_6 > \Omega_4$ for all the glass specimens. The high values obtained for Ω_2 in all glasses indicate that the Ho³⁺ ion is subjected to higher covalency with low symmetry. The spectroscopic quality factor (Ω_4 / Ω_6) related with the rigidity of the glass system has been found to lie between 0.596 and 0.602 in the present glasses.

The values of Judd-Ofelt intensity parameters are given in **Table 5**.

Table 5: Judd-Ofelt intensity parameters for Ho³⁺ doped ZLAABP glass specimens.

Glass Specimen	$\Omega_2(\text{pm}^2)$	$\Omega_4(\text{pm}^2)$	$\Omega_6(\text{pm}^2)$	Ω_4 / Ω_6	Ref.
ZLAABP (HO01)	5.874	1.244	2.066	0.602	P.W.
ZLAABP (HO1.5)	5.696	1.227	2.046	0.600	P.W.
ZLAABP (HO02)	5.377	1.203	2.020	0.596	P.W.
Tellurite(HO)	4.98	0.99	2.96	0.334	[24]

4.4. Fluorescence Spectrum

The fluorescence spectrum of Ho³⁺ doped in zinc lithium alumino antimony borophosphate glass is shown in Figure 4. There are two broad bands observed in the Fluorescence spectrum of Ho³⁺ doped zinc lithium alumino antimony borophosphate glass. The wavelengths of these bands along with their assignments are given in Table 6.

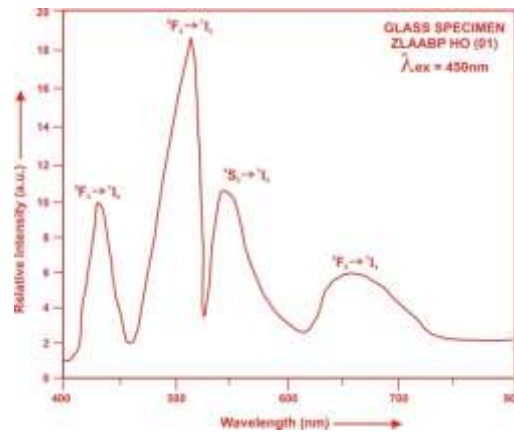


Fig. (4). Fluorescence spectrum of doped with Ho³⁺ ZLAABP glasses.

Table6: Emission peak wave lengths (λ_p),radiative transition probability (A_{rad}),branching ratio (β),stimulated emission cross-section(σ_p) and radiative life time(τ_R) for various transitions in Ho³⁺ doped ZLAABP glasses.

Transition	ZLAABP (HO 01)					ZLAABP (HO1.5)				ZLAABP (HO 02)			
	λ_{max} (nm)	$A_{rad}(s^{-1})$	β	σ_p ($10^{-20} cm^2$)	$\tau_R(\mu s)$	$A_{rad}(s^{-1})$	β	σ_p ($10^{-20} cm^2$)	$\tau_R (\mu s)$	$A_{rad}(s^{-1})$	β	σ_p ($10^{-20} cm^2$)	τ_R ($10^{-20} cm^2$)
⁵ F ₃ → ⁵ I ₈	435	4615.64	0.289 6	0.577	6274.3 5	4583.02	0.2899	0.563	6324.7 2	4528.2 3	0.290 0	0.543	6404.45
⁵ F ₄ → ⁵ I ₈	501	7317.35	0.459 1	1.283		7256.73	0.4590	1.255		7164.4 6	0.458 8	1.223	
⁵ S ₂ → ⁵ I ₈	555	1927.96	0.121 0	0.450		1911.98	0.1210	0.439		1890.4 2	0.121 1	0.428	
⁵ F ₅ → ⁵ I ₈	652	2076.97	0.130 3	0.773		2059.24	0.1302	0.757		2031.0 3	0.130 1	0.736	

V. Conclusion

In the present study, the glass samples of composition (35-x) P₂O₅:10ZnO:10Li₂O:10Al₂O₃:15Sb₂O₃:20B₂O₃:xHo₂O₃ (where x =1, 1.5 and 2mol %) have been prepared by melt-quenching method. The value of stimulated emission cross-section (σ_p) is found to be maximum for the transition (⁵F₄→⁵I₈) for glass ZLAABP (HO 01), suggesting that glass ZLAABP (HO 01) is better compared to the other two glass systems ZLAABP (HO1.5) and ZLAABP (HO02).

References:

[1]. Seshadri, M., Rao, K.V., Koteswara Rao, K.S.R. and Ratnakaram, Y.C., (2010).Spectroscopic investigations and luminescence spectra of Nd³⁺ and Dy³⁺ doped different phosphate glasses, Journal of luminescence 130(4), 536-543.

[2]. Sava, B. A., Elisa,M., Boroica, L. and Monteiro, R.C.C.(2013).Preparation method and thermal properties of samarium and Europium doped alumino phosphate glasses, Material Science and Engineering 178(20),1429-1435.

[3]. Seshadri, M., Radha, M., Barbosa, C., Cordeiro, C.M.B. and Ratnaka, Y.C. (2015).Effect of ZnO on spectroscopic properties of Sm³⁺doped zinc phosphate glasses, Physica B: Condensed matter 459, 79-87.

[4].Wojciench, A., Pisarski, L. Z., Tomasz, G., sottys, M. and Joanna, P. (2014).Structure and Spectroscopy of rare earth doped lead phosphate glasses.(Eu, Tb, Dy, Er), Journal of Alloys and Compound 587, 90-98.

[5]. Chen, Y., Chen, G.H., Liu, X.Y. and Yang, T.(2018).Enhanced up – conversion luminescence and optical thermometry characteristics of Er³⁺/ Yb³⁺ co-doped transparent phosphate Glass Ceramics, Journal of luminescence 195,314-320.

[6]. Mitra, S. and Jana, S. (2015). Intense orange emission in Pr³⁺ doped lead phosphate glass, Journal of physics and chemistry of solids 85,245-253.

[7]. Masai, H., Takahashi, Y., Fujiwara, T., Matsumoto, S. and Yoko T. (2010).High photoluminescent of low melting Sn doped phosphate Glass, Applied physics Express 3(8), 082102.

- [8]. Yaacob, S.N.S., Sahar, M.R., Sazali, E.S., Mahraz, Z. A., Sulhadi, K., Mahraz, Z.A. and Sulhadi, K. (2018). Comprehensive study on compositional modification of Tb³⁺ doped Zinc phosphate Glass, *Solid State Sciences* 81, 51-57.
- [9]. Rai, V.N., Raja Sekhar, B.N., Tiwari, P., Kshirsagar, R.J. and Deb, S.K. (2011). Spectroscopic studies of gamma irradiated Nd³⁺ doped phosphate Glasses, *Journal of Non- crystalline solids*, 3757-3764.
- [10]. Deepa, A.V., Priyamurygasen, P., Muralimanohar, K., Sathyamoorthy, and P., kumar, V. (2019) .A comparison on the structural and optical properties of different rare earth doped phosphate glass, *Optik*, 181,361-367.
- [11]. Linganna, K., SrinivasaRao, Ch. and Jayasankar, C.K.(2013). Optical properties and generation of white light in Dy³⁺ doped lead phosphate glasses, *Journal of Quantitative Spectroscopy and Radiative Transfer*, 118, 40-48.
- [12]. El Maaref, A.A., Shaaban, S. Kh.S., Wahab, E.A. A. and Elokr, M.M. (2019). Optical properties and radiative rates of Nd³⁺ doped zinc- sodium phosphate Glasses, *Journal of rare Earth*, 37, 253-259.
- [13]. S. Areej, Alqarni, S., Hussin, R., Alamri, S.N. and Ghoshal, S.K. (2020). Tailored structures and dielectric traits of holmium ion-doped zinc-sulpho-boro-phosphate glass ceramics, *Ceramics International* 46(3), 3282-3291.
- [14]. Marzouk, M. A., Hamdy, Y. M., Elbatal, H. A. and Ezzeldin, F. M. (2015). Photoluminescence and spectroscopic dependence of fluorophosphates glasses on samarium ions concentration and the induced defects by gamma irradiation, *Journal of Luminescence*, 166, 295–303.
- [15]. Sene, F.F., Maritnelli, J.R. and Gomes, L. (2004). Optical and structural characterization of rare earth doped niobium phosphate glasses, *Journal of Non- Crystalline Solids* 348, 63-71.
- [16]. Gorller-Walrand, C. and Binnemans, K. (1988). Spectral Intensities of f-f Transition. In: Gshneidner Jr., K.A. and Eyring, L., Eds., *Handbook on the Physics and Chemistry of Rare Earths*, Vol. 25, Chap. 167, North-Holland, Amsterdam, 101-264.
- [17]. Sharma, Y.K., Surana, S.S.L. and Singh, R.K. (2009). Spectroscopic Investigations and Luminescence Spectra of Sm³⁺ Doped Soda Lime Silicate Glasses. *Journal of Rare Earths*, 27, 773.
- [18]. Judd, B.R. (1962). Optical Absorption Intensities of Rare Earth Ions. *Physical Review*, 127, 750.
- [19]. Ofelt, G.S. (1962). Intensities of Crystal Spectra of Rare Earth Ions. *The Journal of Chemical Physics*, 37, 511.
- [20]. Sinha, S.P. (1983). Systematics and properties of lanthanides, Reidel, Dordrecht.
- [21]. Krupke, W.F. (1974). *IEEE J. Quantum Electron QE*, 10,450.
- [22] Weinberg, M.C. (1994). Experimental test of surface nucleated crystal growth model in lithium diborate glass, *Phys. Chem. Glasses* 35, 119.
- [23] Lu, Z.P. and Liu, C.T. (2003). Glass Formation Criterion for Various Glass-Forming Systems *Phys. Rev. Lett.* 91,115505.
- [24]. Rai, S.B., Singh, A.K., Singh, S.K., (2003). Spectroscopic properties of Ho³⁺ ions doped in tellurite glass. *Spectrochim. Acta Part A Mol. Biomol. Spectrosc.* 59, 3221– 3226.